Universal Behavior in Entanglement Entropy Reveals Quantum Criticality and Underlying Symmetry Breaking

Zhe Wang[1,2†], Zehui Deng[3†], Zenan Liu[1,2], Zhiyan Wang[1,2], Yi-Ming Ding[1,2], Long Zhang[4*], Wenan Guo[5,6*], and Zheng Yan[1,2*]

[1]*Department of Physics, School of Science and Research Center for Industries of the Future, Westlake University, Hangzhou 310030, China*
[2]*Institute of Natural Sciences, Westlake Institute for Advanced Study, Hangzhou 310024, China*
[3]*Beijing Computational Science Research Center, Beijing 100193, China*
[4]*Kavli Institute for Theoretical Sciences and CAS Center for Excellence in Topological Quantum Computation, University of Chinese Academy of Sciences, Beijing 100190, China*
[5]*School of Physics and Astronomy, Beijing Normal University, Beijing 100875, China*
[6]*Key Laboratory of Multiscale Spin Physics (Ministry of Education), Beijing Normal University, Beijing 100875, China*

(Received 6 August 2025; accepted manuscript online 30 September 2025)

Entanglement plays a key role in quantum physics, but how much information it can extract from many-body systems is still an open question, particularly regarding quantum criticalities and emergent symmetries. In this work, we systematically study the entanglement entropy (EE) and derivative entanglement entropy (DEE) near quantum phase transitions in various quantum many-body systems. A one-parameter scaling relation between the DEE and system size at the critical point has been derived for the first time, which successfully obtains the critical exponent via data collapse. Furthermore, we find that the EE peaks at the (emergent) symmetry-enhanced first-order transition, reflecting higher symmetry breaking. This work provides a new paradigm for quantum many-body research from the perspective of EE and DEE.

DOI: 10.1088/0256-307X/42/11/110712 CSTR: 32039.14.0256-307X.42.11.110712

1. Introduction. The information-theoretic perspective of quantum many-body systems is a blooming interdisciplinary research frontier,[1–4] where the entanglement entropy (EE) plays a pivotal role. For a subsystem embedded in a large system, the EE quantifies the quantum correlations of the subsystem with the rest of the whole system and provides a generic upper bound on local operator correlations.[5] It grows with the subsystem size following the area law at the ground state of a generic short-range correlated system with an energy gap,[5–7] and has a logarithmic enhancement beyond the area law in one-dimensional (1D) quantum critical states described by conformal field theory (CFT)[8–11] and gapless fermion systems with Fermi surfaces in higher dimensions.[12–15] The area law of the EE is the guiding principle for developing of numerical schemes based on matrix-product and tensor network states.[16–19] Moreover, the strong subadditivity of EE was adopted to prove monotonicity of renormalization group (RG) flow in relativistic quantum field theory.[20,21]

In a 2D quantum many-body system with (emergent) Lorentz symmetry, the area law of the EE states that $S(\ell) \sim \alpha\ell$, in which ℓ is the length of the subsystem boundary. The area law of the EE arises from short-range correlations across the boundary in the gapped disordered phase. In addition, it also arises from long-range correlations near a quantum critical point (QCP), where the correlation length diverges. The prefactor α varies with the tuning parameter g in the Hamiltonian and exhibits a cusp singularity at the QCP g_c,[22] $\alpha(g)-\alpha(g_c) \propto |g-g_c|^{\nu}$, where ν is the correlation length critical exponent. Such a cusp singularity has been confirmed through quantum Monte Carlo (QMC) simulations and mean-field theory for (2+1)D QCPs.[23,24] However, a more complete quantum critical scaling form of the EE itself (not only the prefactor α) and its derivative remains largely elusive due to a lack of highly efficient numerical methods for computing the EE in 2D quantum many-body systems.

In this work, we investigate the universal scaling behavior of the EE and its derivative (denoted by DEE) in the vicinity of (2+1)D QCPs. The EE is calculated using the bipartite reweight-annealing QMC scheme developed recently[25–27] by applying a reweight-annealing procedure[28,29] along the path of real physical parameters, which enables a high-throughput scan of the EE near the QCP. While the cusp singularity of the EE is at the same order as its nonsingular part, we observe a stronger singularity in the DEE data near the QCP. We propose a univer-

†These authors contributed equally to this work.
*Corresponding authors. Email: longzhang@ucas.ac.cn; waguo@bnu.edu.cn; zhengyan@westlake.edu.cn
© 2025 Chinese Physical Society and IOP Publishing Ltd. All rights, including for text and data mining, AI training, and similar technologies, are reserved.

sal one-parameter scaling relation for the DEE in Eq. (2), which is corroborated by the data collapse near (2+1)D QCPs in the O(N) ($1 \leq N \leq 3$) universality classes. The scaling relation fails for first-order quantum phase transitions; nonetheless, we find that the EE shows a peak at the first-order transition that spontaneously breaks an enhanced continuous symmetry, which can be attributed to the larger number of Goldstone modes at the transition. Therefore, our work demonstrates that both EE and DEE are useful information-theoretic measures of quantum phase transitions.

2. Models and Method. We will focus on quantum spin models with QCPs in the (2+1)D O(N) ($1 \leq N \leq 3$) universality classes. We also study the symmetry-enhanced first-order transitions for comparison. The model Hamiltonians are illustrated in Fig. 1 and described in detail in the following sections. Numerical simulations are performed on $L_x \times L_y$ square lattice with periodic boundary conditions in both directions. Considering the dynamical critical exponent $z = 1$ in this work, the inverse temperature increases linearly with the lattice size, $\beta = L_x$, to approach the quantum critical regime. The subsystem is a $(L_x/2) \times L_y$ cylinder region with two smooth boundaries, and the total boundary length $\ell = 2L_y$. We adopt the bipartite reweight-annealing algorithm [25] combined with stochastic series expansion QMC simulations [30–35] to extract the second Rényi EE of the subsystem, $S^{(2)} = -\ln \mathrm{tr}\rho_A^2$, where ρ_A is the reduced density matrix. The calculation details are presented in the Supplementary Materials (SM).*

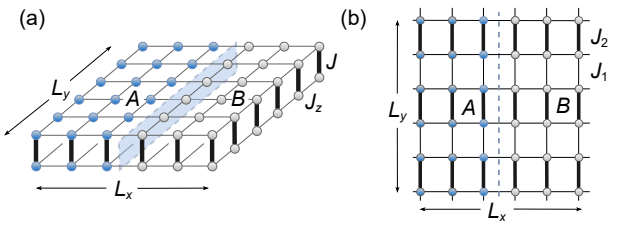

Fig. 1. Quantum spin models on a square lattice with periodic boundary conditions. The lattice size is $L_x \times L_y$, and the subsystem is a $(L_x/2) \times L_y$ cylinder region, which is separated from the rest part by the dashed lines. (a) Spin-1/2 bilayer Ising–Heisenberg model. $-J_z < 0$ denotes the intralayer FM Ising interaction, while $J > 0$ is the interlayer AF Heisenberg interaction. (b) Spin-1/2 dimerized Heisenberg model. The AF interaction strengths on the thin and the thick bonds are J_1 and J_2, respectively. The anisotropy parameter Δ is the same on all bonds.

3. Universal Scaling Relation. Let us first derive a universal quantum critical scaling form for the EE and its derivative, which is valid for both the Rényi EE and the von Neumann EE. In the quantum critical regime, the EE is contributed to by both nonsingular short-range correlations and singular long-range correlations. For a subsystem with a smooth boundary, the EE near the QCP is given by [22]

$$S(\ell, g) = a(g)\ell + \tilde{S}_0(x), \tag{1}$$

where ℓ is the boundary length. The prefactor $a(g)$ in the first term varies analytically with the tuning parameter g, while $\tilde{S}_0$ is a universal function of the dimensionless scaling variable $x = (g - g_c)\ell^{1/\nu}$.† At the QCP, the $\tilde{S}_0$ term reduces to a universal constant, which depends only on the universality class of the QCP and the geometric invariants of the subsystem, e.g., the aspect ratio of the cylinder region. Away from the QCP, the $\tilde{S}_0$ term also contributes to the area law, $\tilde{S}_0(x) = r|g - g_c|^\nu \ell$ for $|x| \gg 1$, in which r is a constant coefficient, thus leading to a cusp singularity of the area-law prefactor, $\alpha(g) = a(g) + r|g - g_c|^\nu$. [22] Therefore, both terms in Eq. (1) are of the same order in the limit as $\ell \to \infty$ and are difficult to be clearly separated in numerical analysis.

From our numerical results shown in Fig. 2, we observe that the derivative of the EE with respect to the tuning parameter $\partial S(\ell, g)/\partial g$ exhibits a stronger singularity near the QCP. From Eq. (1), we find

$$\frac{\partial S(\ell, g)}{\partial g} = a'(g)\ell + \tilde{S}_0'(x)\ell^{1/\nu}. \tag{2}$$

For the (2+1)D O(N) ($1 \leq N \leq 3$) models studied in this work, the critical exponent $\nu < 1$, thus the second term in Eq. (2) derived from the critical behavior dominates in the limit as $\ell \to \infty$. Therefore, the DEE is a better diagnosis of the universal scaling behavior of the quantum entanglement in the quantum critical regime. The scaling function $\tilde{S}_0'(x)$ can be expanded into a polynomial near the QCP,

$$\tilde{S}_0'(x) = \sum_{k=0}^{k_{\max}} \frac{1}{k!} \tilde{S}_0^{(k+1)}(0) x^k. \tag{3}$$

The first term in Eq. (2) serves as a subleading correction to the scaling relation of the DEE. The prefactor $a'(g)$ can be expanded into a power series in general,

$$a'(g) = a'(g_c) + a''(g_c)(g - g_c) + \cdots, \tag{4}$$

and we find it suffices to retain only the constant term in practice. The critical point g_c, the critical exponent ν, and the coefficients $\tilde{S}_0^{(k+1)}(0)$ and $a'(g_c)$ are the fitting parameters in the following data collapse analysis.

4. Ising Transition. Let us focus on the spin-1/2 bilayer Ising–Heisenberg model shown in Fig. 1(a). Its Hamiltonian is given by [36]

$$H = -J_z \sum_{\alpha=1,2} \sum_{\langle ij \rangle} S_{i,\alpha}^z S_{j,\alpha}^z + J \sum_i \boldsymbol{S}_{i,1} \cdot \boldsymbol{S}_{i,2}, \tag{5}$$

where α is the layer index, and $\langle ij \rangle$ denotes the summation

*See the SM for further details of the reweight-annealing algorithm for the Rényi EE, the definition of the checkerboard J–Q model, and our failed attempts at data collapse analysis of the EE near QCPs and the derivative of EE near first-order transitions, and Ref. [76].

†The universal scaling function in the EE was denoted by $S_0(\ell/\xi)$ as a function of the dimensionless ratio ℓ/ξ in Ref. [22], in which $\xi \propto |g - g_c|^{-\nu}$ is the correlation length. Here, we introduce the scaling variable $x = (g - g_c)\ell^{1/\nu} \propto (\ell/\xi)^{1/\nu}$ to facilitate further analysis.

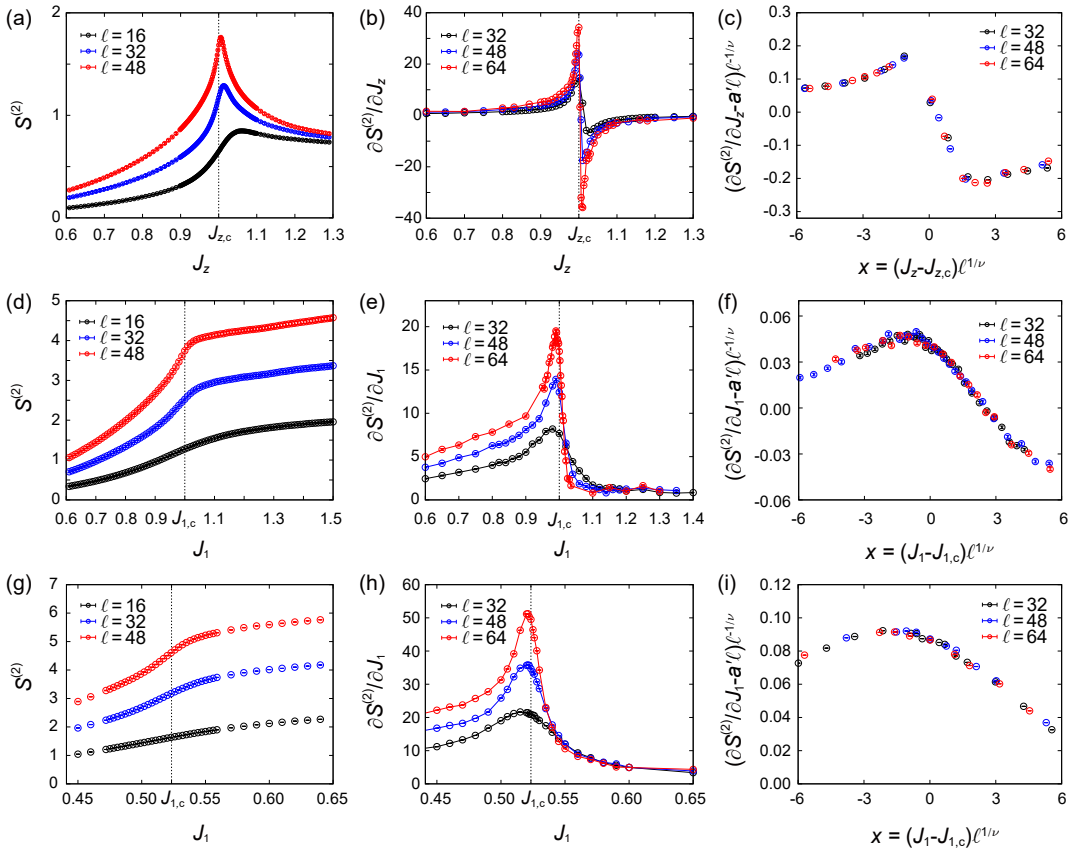

Fig. 2. (a) The second Rényi EE and (b) its derivative, and (c) the scaling function $\tilde{S}_0'(x)$ obtained from the data collapse analysis of the DEE near the Ising transition of the bilayer Ising–Heisenberg model. In the calculations, $J = 3.045$ is fixed, while J_z is tuned near the QCP $J_{z,c} = 1$. (d)–(f) Data for the dimerized Heisenberg model with an anisotropy parameter $\Delta = 0.9$. $J_2 = 2.1035$ is fixed, while J_1 is tuned around the O(2) QCP $J_{1,c} = 1$. (g)–(i) Data for the dimerized isotropic Heisenberg model. $J_2 = 1$ is fixed, while J_1 is tuned around the O(3) QCP $J_{1,c} = 0.52337$.

over nearest-neighbor bonds within each layer. $-J_z < 0$ is the intralayer ferromagnetic (FM) Ising interaction, while $J > 0$ is the interlayer antiferromagnetic (AF) Heisenberg interaction. For $J/J_z \ll 1$, the ground state has an intralayer-FM-interlayer-AF order, which breaks the $\mathbb{Z}_2$ spin flip symmetry generated by $X = \prod_{i,\alpha} \sigma^x_{i,\alpha}$. For $J/J_z \gg 1$, the ground state approaches a direct product of interlayer spin-singlet states, which has an energy gap and does not break any symmetries. The QCP separating these two phases is located at $J/J_z = 3.045(2)$ and belongs to the (2+1)D Ising universality class.[36]

Fixing $J = 3.045$ and tuning J_z around the QCP $J_{z,c} = 1$, we evaluate the second Rényi EE and its derivative for different lattice sizes. The results are plotted in Figs. 2(a) and 2(b). The EE shows a maximum at the QCP, thus the DEE changes sign across the QCP. The maximum of the EE can be attributed to the stronger spatial correlations in the quantum critical state than in the adjacent gapped phases.

We cannot achieve a satisfactory data collapse for the EE data with the dimensionless scaling variable $x = (J_z - J_{z,c})\ell^{1/\nu*}$, because the singular and the nonsingular contributions are of the same order as we argued before. Nonetheless, the stronger singularity in the DEE data motivates us to perform scaling analysis on the DEE. In this case, it is difficult to capture the scaling function $\tilde{S}_0'(x)$ with a single (low-order) polynomial on both sides of the QCP due to the abrupt sign change of the DEE. Hence, we first fit the scaling relation Eq. (2) to the DEE data on the right-hand side of the QCP ($J_z > 1$) and obtain $J_{z,c} = 1.003(1)$ and $\nu = 0.62(7)$. Meanwhile, we find the DEE data on the left-hand side ($J_z < 1$) also collapse perfectly onto a single curve of the scaling variable x with the same $J_{z,c}$ and ν [see Fig. 2(c)]. Moreover, these values are fully consistent with the QCP $J_{z,c} = 1$ in Ref. [36] and the critical exponent $\nu = 0.63012$ of the (2+1)D Ising universality class.[36–38] The scaling function $\tilde{S}_0'(x)$ obtained from the data collapse analysis is shown in Fig. 2(c).

5. Continuous Symmetry Breaking Transitions. We then study the spin-1/2 dimerized Heisenberg model illustrated in Fig. 1(b). The Hamiltonian is given by[39,40]

$$H = J_1 \sum_{\langle ij \rangle} D_{ij} + J_2 \sum_{\langle ij \rangle'} D_{ij}, \tag{6}$$

where the summation in the J_1-term is taken over the thin bonds, while the J_2-term is over the thick bonds. The nearest-neighbor AF Heisenberg interaction $D_{ij} = S^x_i S^x_j + S^y_i S^y_j + \Delta S^z_i S^z_j$ is in general anisotropic, and we

consider a spatially uniform anisotropy Δ in the range $0 < \Delta \leq 1$. In the $J_2/J_1 \simeq 1$ regime, the ground state has a long-range AF order. For $0 < \Delta < 1$, the AF order parameter lies in the xy-plane and breaks the O(2) spin rotation symmetry, while for $\Delta = 1$, the interaction is isotropic, and the AF order breaks the O(3) symmetry. In the $J_2/J_1 \gg 1$ limit, the ground state approaches a direct product of the spin-singlet states on the thick bonds, which has an energy gap and does not break any symmetries. The QCP separating the gapped phase and the AF ordered phase belongs to the (2+1)D O(2) ($0 < \Delta < 1$) or the O(3) ($\Delta = 1$) universality class.

The second Rényi EE and its derivative are evaluated around the QCPs in the easy-plane case ($\Delta = 0.9$) and in the isotropic case ($\Delta = 1$). The results are plotted in Figs. 2(d), 2(e), 2(g), and 2(h), respectively. In each case, we fix J_2 and tune J_1 around the QCP as described in the figure caption. We find the EE grows monotonically from the gapped phase across the QCP to the AF-ordered phase, which is quite different from the Ising transition case. This indicates that quantum correlations in the AF ordered phase are even stronger than at the QCP, which can be attributed to the gapless Goldstone modes (spin waves) due to the continuous symmetry breaking.[41–43] Similar behavior was observed near the QCP of the bilayer Heisenberg model in the (2+1)D O(3) universality class.[23]

Similar to the Ising transition case, we cannot achieve a satisfactory data collapse for the EE either.* Thus, we turn to the DEE. Fitting the scaling relation Eq. (2) to the DEE data, we find $J_{1,c} = 0.997(2)$ and $\nu = 0.66(2)$ in the easy-plane case ($\Delta = 0.9$), and $J_{1,c} = 0.523(1)$ and $\nu = 0.71(4)$ in the isotropic case ($\Delta = 1$). These results are fully consistent with the known QCPs and the critical exponents: $J_{1,c} = 1$ and $\nu = 0.6703$ for the O(2) transition ($\Delta = 0.9$), and $J_{1,c} = 0.52337$ and $\nu = 0.7073$ for the O(3) transition ($\Delta = 1$).[37,39,40,44] The scaling functions $\tilde{S}_0(x)$ obtained from the data collapse analysis are plotted in Figs. 2(f)–2(i).

6. Symmetry-Enhanced First-Order Transitions. Having established the universal scaling relation of the DEE near (2+1)D QCPs, we examine the first-order quantum phase transitions with enhanced symmetries for comparison.

Let us first study the 2D anisotropic Heisenberg model given in Eq. (6) with a spatially uniform AF interaction $J_1 = J_2 = 1$, and take the anisotropy Δ as a tuning parameter. At $\Delta = 1$, the Heisenberg interaction is isotropic with an O(3) symmetry, which is spontaneously broken by the AF order at the ground state. Away from this point, the symmetry is explicitly reduced to $\mathrm{O}(2) = \mathrm{SO}(2) \rtimes \mathbb{Z}_2$ generated by uniaxial spin rotation and spin-flip transformations. For $0 < \Delta < 1$, the ground state has an easy-plane AF order and breaks SO(2) spin rotation symmetry, while for $\Delta > 1$, the ground state has an easy-axis AF order and breaks $\mathbb{Z}_2$ spin flip symmetry. The easy-plane and the easy-axis AF order parameters coexist at $\Delta = 1$ and jump to zero across the transition; hence, this is a first-order transition with a spontaneously broken enhanced symmetry.[45]

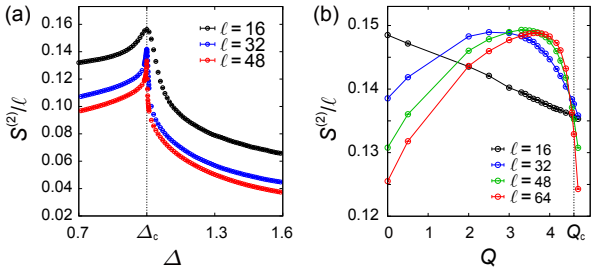

Fig. 3. The second Rényi EE divided by the boundary length $S^{(2)}/\ell$ of (a) the anisotropic Heisenberg model and (b) the checkerboard J–Q model near the symmetry-enhanced first-order transitions.

The second Rényi EE near the transition is plotted in Fig. 3(a). It shows a sharp peak at the transition point, indicating stronger quantum correlations than those in the adjacent phases, which can be attributed to the larger number of Goldstone modes and low-energy density of states (DOS) at the transition point. We cannot achieve a satisfactory data collapse for the DEE data,* which is not surprising given the first-order nature of the transition.

The symmetry-enhanced first-order transition is not restricted to systems with exact symmetries. An enhanced symmetry can emerge in the long-wavelength limit if all explicit symmetry-breaking interactions are irrelevant and diminish with the RG flow. Such an enhanced symmetry can even emerge at a first-order transition between two ordered phases. At the putative deconfined QCP between the AF order and the valence-bond solid (VBS) order[46,47] in the J–Q model,[48,49] an emergent SO(5) symmetry of the AF and the VBS order parameters was observed.[50–52] While theoretical arguments[46,47,53] and early numerical results[48,49] suggested a continuous quantum phase transition, anomalous scaling behavior was observed in various physical quantities, and its origin has been debated for a long time.[54–61] Recently, the anomalous logarithmic correction term in the EE at the transition[62–66] has been observed; it is attributed to Goldstone modes associated with continuous symmetry breaking. The number of Goldstone modes is consistent with the spontaneous breaking of an (emergent) SO(5) symmetry. Hence, it supports the symmetry-enhanced first-order transition scenario.[67]

We study the checkerboard J–Q model on a square lattice, which has a first-order transition between the O(3)-symmetry-breaking AF order and the $\mathbb{Z}_2$-symmetry-breaking plaquette-singlet solid (PSS) order at $Q_c/J = 4.598(1)$.[45]* At the transition point, an enhanced O(4) symmetry among the AF and the PSS order parameters emerges and is spontaneously broken at the ground state.[45] Its Rényi EE near the transition point is plotted in Fig. 3(b). The EE shows a broad peak, which progressively moves to the transition point as the lattice size increases. This is qualitatively consistent with the spontaneous breaking of the enhanced symmetry with more Gold-

stone modes and low-energy DOS at the transition than in adjacent AF and PSS phases. The drift of the peak implies that enhanced symmetry is not exact but emergent with RG flow. Specifically, there exists a relatively large irrelevant field, which typically scales as a negative power of system size. As system size increases, the effect of this irrelevant field gradually vanishes. Consequently, we observe that peak position corresponding to enhanced symmetry shifts with increasing system size. This is also reflected in the fact that as system size increases, width of peak gradually narrows. In thermodynamic limit, it should evolve into a sharp peak.

The relationship of the EE and the low-energy DOS can be explained further based on the correspondence between the entanglement spectrum (ES) and the low-energy spectrum of the subsystem with a boundary. Such a correspondence was first demonstrated [68,69] for topological states with gapless boundary, and was also rigorously proved in (1+1)D CFT. [70–72] Recently, such a correspondence was put forward in a more general setting based on the "wormhole picture" in the path integral formulation of the reduced density matrix and verified with numerical simulations. [73–75] Thereby, a larger low-energy DOS from the Goldstone modes implies a denser low-energy ES and hence a larger EE.

7. Conclusion and Discussions. We have systematically studied the EE and its derivative around quantum phase transitions in 2D quantum many-body systems. In the quantum critical regime, although the singular and the nonsingular terms in the EE are of the same order and cannot be clearly separated, the DEE shows a stronger singularity induced by the quantum criticality. We have obtained a universal scaling relation for the DEE, and corroborated it with the data collapse near (2+1)D QCPs. The scaling relation fails for first-order transitions; Nonetheless, the EE shows a peak at symmetry-enhanced first-order transitions, which can be attributed to the larger low-energy DOS from the Goldstone modes.

The EE is a basis-independent measure of generic quantum correlations, hence it does not require a prior knowledge of the quantum phase transitions and should be particularly suitable for detecting exotic QCPs beyond the conventional paradigm of spontaneous symmetry breaking. Other information-theoretic measures of quantum many-body systems may also be explored to characterize quantum critical phenomena in the future.

Acknowledgements. We thank the helpful discussions with Marchello Delmonte, Yan-Cheng Wang, Yin Tang, and Wei Zhu. This work was supported by the the National Natural Science Foundation of China (Grant Nos. 12175015 for W.G. and 12174387 for L.Z.), the Chinese Academy of Sciences (Grant Nos. YSBR-057 and JZHKYPT-2021-08 for L.Z.), the Innovative Program for Quantum Science and Technology (Grant No. 2021ZD0302600 for L.Z.), and the start-up funding of Westlake University and the China Postdoctoral Science Foundation (Grant No. 2024M752898 for Z.W. and Z.Y.). The authors thank the high-performance computing center of Westlake University and the Beijing PARATERA Tech Co., Ltd. for providing HPC resources.

References

[1] Amico L, Fazio R, Osterloh A, and Vedral V 2008 *Rev. Mod. Phys.* **80** 517
[2] Eisert J, Cramer M, and Plenio M B 2010 *Rev. Mod. Phys.* **82** 277
[3] Laflorencie N 2016 *Phys. Rep.* **646** 1
[4] Zeng B, Chen X, Zhou D L, and Wen X G 2019 *Quantum Information Meets Quantum Matter Quantum Science and Technology* (New York, NY: Springer New York)
[5] Wolf M M, Verstraete F, Hastings M B, and Cirac J I 2008 *Phys. Rev. Lett.* **100** 070502
[6] Hastings M B 2007 *J. Stat. Mech. Theory Exp.* **2007** P08024
[7] Hastings M B 2007 *Phys. Rev. B* **76** 035114
[8] Holzhey C, Larsen F, and Wilczek F 1994 *Nucl. Phys. B* **424** 443
[9] Vidal G, Latorre J I, Rico E, and Kitaev A 2003 *Phys. Rev. Lett.* **90** 227902
[10] Korepin V 2004 *Phys. Rev. Lett.* **92** 096402
[11] Calabrese P and Cardy J 2004 *J. Stat. Mech.* **2004** P06002
[12] Wolf M M 2006 *Phys. Rev. Lett.* **96** 010404
[13] Gioev D and Klich I 2006 *Phys. Rev. Lett.* **96** 100503
[14] Ding W, Seidel A, and Yang K 2012 *Phys. Rev. X* **2** 011012
[15] Jiang W, Pan G, Wang Z, Mao B B, Shen H, and Yan Z 2024 arXiv:2409.20009 [cond-mat.stat-mech]
[16] Verstraete F, Popp M, and Cirac J I 2004 *Phys. Rev. Lett.* **92** 027901
[17] Verstraete F, Murg V, and Cirac J 2008 *Adv. Phys.* **57** 143
[18] Schollwöck U 2011 *Ann. Phys.* **326** 96
[19] Cirac J I, Pérez-García D, Schuch N, and Verstraete F 2021 *Rev. Mod. Phys.* **93** 045003
[20] Casini H and Huerta M 2007 *J. Phys. A Math. Theor.* **40** 7031
[21] Casini H and Huerta M 2012 *Phys. Rev. D* **85** 125016
[22] Metlitski M A, Fuertes C A, and Sachdev S 2009 *Phys. Rev. B* **80** 115122
[23] Helmes J and Wessel S 2014 *Phys. Rev. B* **89** 245120
[24] Frérot I and Roscilde T 2016 *Phys. Rev. Lett.* **116** 190401
[25] Wang Z, Wang Z, Ding Y M, Mao B B, and Yan Z 2025 arXiv:2406.05324 [cond-mat.str-el]
[26] Ding Y M, Tang Y, Wang Z, Wang Z, Mao B B, and Yan Z 2024 arXiv:2409.10273 [cond-mat.str-el]
[27] Wang Z, Liu Z, Wang Z, and Yan Z 2024 arXiv:2412.01384 [cond-mat.str-el]
[28] Ding Y M, Sun J S, Ma N, Pan G, Cheng C, and Yan Z 2024 *Phys. Rev. B* **110** 165152
[29] Ma N, Sun J S, Pan G, Cheng C, and Yan Z 2024 *Phys. Rev. B* **110** 125141
[30] Sandvik A W 1992 *J. Phys. A* **25** 3667
[31] Sandvik A W 1999 *Phys. Rev. B* **59** R14157
[32] Syljuåsen O F and Sandvik A W 2002 *Phys. Rev. E* **66** 046701
[33] Sandvik A W and Evertz H G 2010 *Phys. Rev. B* **82** 024407
[34] Yan Z, Wu Y, Liu C, Syljuåsen O F, Lou J, and Chen Y 2019 *Phys. Rev. B* **99** 165135
[35] Yan Z 2022 *Phys. Rev. B* **105** 184432
[36] Wu S, Ran X, Yin B, Li Q F, Mao B B, Wang Y C, and Yan Z 2023 *Phys. Rev. B* **107** 155121
[37] Guida R and Zinn-Justin J 1998 *J. Phys. A. Math. Gen.* **31** 8103
[38] Deng Y and Blöte H W J 2003 *Phys. Rev. E* **68** 036125

[39] Matsumoto M, Yasuda C, Todo S, and Takayama H 2001 *Phys. Rev. B* **65** 014407
[40] Zhu W, Ding C, Zhang L, and Guo W 2022 arXiv:2111.12336 [cond-mat.str-el]
[41] Song H F, Flindt C, Rachel S, Klich I, and Le Hur K 2011 *Phys. Rev. B* **83** 161408
[42] Kallin A B, Hastings M B, Melko R G, and Singh R R P 2011 *Phys. Rev. B* **84** 165134
[43] Metlitski M A and Grover T 2015 arXiv:1112.5166 [cond-mat.str-el]
[44] Zhang L and Wang F 2017 *Phys. Rev. Lett.* **118** 087201
[45] Zhao B, Weinberg P, and Sandvik A W 2019 *Nat. Phys.* **15** 678
[46] Senthil T, Vishwanath A, Balents L, Sachdev S, and Fisher M P A 2004 *Science* **303** 1490
[47] Senthil T, Balents L, Sachdev S, Vishwanath A, and Fisher M P A 2004 *Phys. Rev. B* **70** 144407
[48] Sandvik A W 2007 *Phys. Rev. Lett.* **98** 227202
[49] Lou J, Sandvik A W, and Kawashima N 2009 *Phys. Rev. B* **80** 180414
[50] Nahum A, Serna P, Chalker J T, Ortuño M, and Somoza A M 2015 *Phys. Rev. Lett.* **115** 267203
[51] Takahashi J and Sandvik A W 2020 *Phys. Rev. Res.* **2** 033459
[52] Takahashi J, Shao H, Zhao B, Guo W, and Sandvik A W 2024 arXiv:2405.06607 [cond-mat.str-el]
[53] Senthil T and Fisher M P A 2006 *Phys. Rev. B* **74** 064405
[54] Kuklov A B, Matsumoto M, Prokof'ev N V, Svistunov B V, and Troyer M 2008 *Phys. Rev. Lett.* **101** 050405
[55] Jiang F J, Nyfeler M, Chandrasekharan S, and Wiese U J 2008 *J. Stat. Mech. Theory Exp.* **2008** P02009
[56] Sandvik A W 2010 *Phys. Rev. Lett.* **104** 177201
[57] Chen K, Huang Y, Deng Y, Kuklov A B, Prokof'ev N V, and Svistunov B V 2013 *Phys. Rev. Lett.* **110** 185701
[58] Shao H, Guo W, and Sandvik A W 2016 *Science* **352** 213
[59] Zhao B, Takahashi J, and Sandvik A W 2020 *Phys. Rev. Lett.* **125** 257204
[60] Sandvik A W and Zhao B 2020 *Chin. Phys. Lett.* **37** 057502
[61] D'Emidio J, Eberharter A, and Läuchli A 2023 *SciPost Phys.* **15** 061
[62] Zhao J, Wang Y C, Yan Z, Cheng M, and Meng Z Y 2022 *Phys. Rev. Lett.* **128** 010601
[63] Song M, Zhao J, Cheng M, Xu C, Scherer M M, Janssen L, and Meng Z Y2025 arXiv:2307.02547 [cond-mat.str-el]
[64] Liao Y D, Pan G, Jiang W, Qi Y, and Meng Z Y2023 arXiv:2302.11742 [cond-mat.str-el]
[65] D'Emidio J and Sandvik A W 2024 *Phys. Rev. Lett.* **133** 166702
[66] Song M, Zhao J, Meng Z Y, Xu C, and Cheng M 2024 *SciPost Phys.* **17** 010
[67] Deng Z, Liu L, Guo W, and Lin H Q 2024 *Phys. Rev. Lett.* **133** 100402
[68] Li H and Haldane F D M 2008 *Phys. Rev. Lett.* **101** 010504
[69] Qi X L, Katsura H, and Ludwig A 2012 *Phys. Rev. Lett.* **108** 196402
[70] Läuchli A M 2013 arXiv:1303.0741 [cond-mat.stat-mech]
[71] Cardy J and Tonni E 2016 *J. Stat. Mech.* **2016** 123103
[72] Yu X J, Huang R Z, Song H H, Xu L, Ding C, and Zhang L 2022 *Phys. Rev. Lett.* **129** 210601
[73] Yan Z and Meng Z Y 2023 *Nat. Commun.* **14** 2360
[74] Song M, Zhao J, Yan Z, and Meng Z Y 2023 *Phys. Rev. B* **108** 075114
[75] Liu Z, Huang R Z, Yan Z, and Yao D X 2024 *Phys. Rev. B* **109** 094416
[76] Huang R Z and Peng C 2024 arXiv:2405.10230 [cond-mat.str-el]